An Ensemble Deep Learning Algorithm for Structural Heart Disease Screening Using Electrocardiographic Images: PRESENT SHD

Short Title: AI for ECG Image-based Structural Heart Disease Screening

Lovedeep S Dhingra MBBS[a], Arya Aminorroaya MD, MPH[a], Veer Sangha BS[a,b], Aline F Pedroso PhD[a], Sumukh Vasisht Shankar MS[a], Andreas Coppi PhD[c], Murilo Foppa MD, PhD[d], Luisa CC Brant MD, PhD[e,f], Sandhi M Barreto MD, PhD[g], Antonio Luiz P Ribeiro MD, PhD[e,f], Harlan M Krumholz MD, SM[a,h,i], Evangelos K Oikonomou MD, DPhil[a], Rohan Khera MD, MS[a,h,j,k]

[a]Section of Cardiovascular Medicine, Department of Internal Medicine, Yale School of Medicine, New Haven, CT, USA
[b]Department of Engineering Science, University of Oxford, Oxford, UK
[c]Center for Outcomes Research and Evaluation, Yale-New Haven Hospital, New Haven, CT, USA
[d]School of Medicine, Universidade Federal do Rio Grande do Sul, Porto Alegre, Brazil
[e]Department of Internal Medicine, Faculdade de Medicina, Universidade Federal de Minas Gerais, Belo Horizonte, Brazil
[f]Telehealth Center and Cardiology Service, Hospital das Clínicas, Universidade Federal de Minas Gerais, Belo Horizonte, Brazil
[g]Department of Preventive Medicine, School of Medicine, Faculdade de Medicina, Universidade Federal de Minas Gerais, Belo Horizonte, Brazil
[h]Center for Outcomes Research and Evaluation (CORE), Yale New Haven Hospital, New Haven, CT, USA
[i]Department of Health Policy and Management, Yale School of Public Health, New Haven, CT, USA
[j]Section of Biomedical Informatics and Data Science, Yale School of Medicine, New Haven, CT, USA
[k]Section of Health Informatics, Department of Biostatistics, Yale School of Public Health, New Haven, CT, USA

Correspondence to:
Rohan Khera, MD, MS
195 Church Street, 6th Floor, New Haven, CT 06510
rohan.khera@yale.edu

Word Count: 3558
Abstract Word Count: 345
Figures/Tables: 3 Figures/2 Tables

Keywords: Artificial Intelligence; Deep Learning; Structural Heart Disease; Predictive Modeling; Electrocardiograms, Cardiovascular Screening; Echocardiography

ABSTRACT

Background: Identifying structural heart diseases (SHDs) early can change the
course of the disease, but their diagnosis requires cardiac imaging, which is limited
in accessibility.

Objective: To leverage images of 12-lead ECGs for automated detection and
prediction of multiple SHDs using an ensemble deep learning approach.

Methods: We developed a series of convolutional neural network models for
detecting a range of individual SHDs from images of ECGs with SHDs defined by
transthoracic echocardiograms (TTEs) performed within 30 days of the ECG at the
Yale New Haven Hospital (YNHH). SHDs were defined based on TTEs with LV
ejection fraction <40%, moderate-to-severe left-sided valvular disease (aortic/mitral
stenosis or regurgitation), or severe left ventricular hypertrophy (IVSd > 1.5cm and
diastolic dysfunction). We developed an ensemble XGBoost model, PRESENT-SHD,
as a composite screen across all SHDs. We validated PRESENT-SHD at 4 US
hospitals and a prospective population-based cohort study, the Brazilian Longitudinal
Study of Adult Health (ELSA-Brasil), with concurrent protocolized ECGs and TTEs.
We also used PRESENT-SHD for risk stratification of new-onset SHD or heart failure
(HF) in clinical cohorts and the population-based UK Biobank (UKB).

Results: The models were developed using 261,228 ECGs from 93,693 YNHH
patients and evaluated on a single ECG from 11,023 individuals at YNHH (19% with
SHD), 44,591 across external hospitals (20-27% with SHD), and 3,014 in the ELSA-
Brasil (3% with SHD). In the held-out test set, PRESENT-SHD demonstrated an
AUROC of 0.886 (0.877-894), sensitivity of 90%, and specificity of 66%. At hospital-
based sites, PRESENT-SHD had AUROCs ranging from 0.854-0.900, with
sensitivities and specificities of 93-96% and 51-56%, respectively. The model

generalized well to ELSA-Brasil (AUROC, 0.853 [0.811-0.897], sensitivity 88%,

specificity 62%). PRESENT-SHD performance was consistent across demographic

subgroups and novel ECG formats. A positive PRESENT-SHD screen portended a

2- to 4-fold higher risk of new-onset SHD/HF, independent of demographics,

comorbidities, and the competing risk of death across clinical sites and UKB, with

high predictive discrimination.

Conclusion: We developed and validated PRESENT-SHD, an AI-ECG tool

identifying a range of SHD using images of 12-lead ECGs, representing a robust,

scalable, and accessible modality for automated SHD screening and risk

stratification.

CONDENSED ABSTRACT

Screening for structural heart disorders (SHDs) requires cardiac imaging, which has limited accessibility. To leverage 12-lead ECG images for automated detection and prediction of multiple SHDs, we developed PRESENT-SHD, an ensemble deep learning model. PRESENT-SHD demonstrated excellent performance in detecting SHDs across 5 US hospitals and a population-based cohort in Brazil. The model successfully predicted the risk of new-onset SHD or heart failure in both US clinical cohorts and the community-based UK Biobank. By using ubiquitous ECG images to predict a composite outcome of multiple SHDs, PRESENT-SHD establishes a scalable paradigm for cardiovascular screening and risk stratification.

BACKGROUND

Structural heart diseases (SHDs) represent a spectrum of prevalent cardiac
disorders with a long presymptomatic course and with substantially elevated risk of
heart failure (HF) and premature death.[1] The detection of these disorders has
traditionally required advanced cardiac imaging, including echocardiography and
cardiac magnetic resonance imaging, which are resource-intensive and, therefore,
not suitable for large-scale disease screening.[2,3] Consequently, these conditions are
often diagnosed after the development of clinical symptoms, leading to poor health
outcomes.[4–6] Moreover, there are no strategies to identify individuals at risk of
developing SHDs, despite the presence of evidence-based interventions that can
alter the course of patients.[6–8] Thus, there is an urgent need for the development of
an automated, accessible, and scalable strategy for the screening and risk
stratification of SHDs.[1,9]

Previously applications of artificial intelligence for electrocardiograms (AI-
ECG) have shown potential to detect signatures of SHDs.[10–18] A key challenge of AI-
ECG models in detecting specific cardiac disorders using ECGs is the low precision
driven by the low prevalence of individual disorders.[10–12] To overcome this limitation,
ensemble models for detecting a composite of multiple SHDs have been proposed.[19]
Nonetheless, these models use raw ECG voltage data as inputs, which are
inaccessible to clinicians at the point of care and often require modifications to the
technical infrastructure to account for vendor-specific data formats.[19] This precludes
the widespread use of AI-ECG approaches for broad cardiovascular screening, as
these data integrations are not commonly available. Further, most AI-ECG
approaches focus on cross-sectional detection and do not quantify the risk of new-
onset disease in those without SHD, which would identify a group for continued

monitoring. Thus, there is a critical unmet need for an AI-ECG-based strategy to enable cross-sectional detection and longitudinal prediction of multiple SHDs simultaneously using ubiquitous, interoperable, and accessible data input in the form of ECG images.

In this study, we report the development and multinational validation of an ensemble deep learning approach that uses an image of a 12-lead ECG, independent of the format, for the accurate detection and prediction of multiple SHDs.

METHODS

The Yale Institutional Review Board approved the study protocol and waived the need for informed consent as the study involves secondary analysis of pre-existing data. An online version of the model is publicly available for research use at https://www.cards-lab.org/present-shd.

Data Sources

For model development, we included data from the Yale New Haven Hospital (YNHH) during 2015-2023. YNHH is a large 1500-bed tertiary medical center that provides care to a diverse patient population across Connecticut. For external validation of our approach to detect SHDs, we included multiple clinically and geographically diverse cohorts: (i) 4 distinct community hospitals in the Yale-New Haven Health System, the Bridgeport Hospital, Greenwich Hospital, Lawrence + Memorial Hospital, and Westerly Hospital, and (ii) a community-based cohort of individuals in Brazil with protocolized concurrent ECG and TTE assessments, the ELSA-Brasil study.

To evaluate the longitudinal prediction of SHD in people without baseline disease, in addition to serial monitoring data from hospitals in the Yale-New Haven Health System, we included data from the UK Biobank (UKB). UKB is the largest population-based cohort with protocolized ECG assessments and clinical encounters derived from the integrated EHR of the National Health Service in the UK. An overview of all data sources is included in the **Supplementary Methods**.

Study Population for SHD Detection

At YNHH, we identified all adults (≥18 years) who underwent a 12-lead ECG within 30 days of a transthoracic echocardiogram (TTE), excluding those with prior cardiac surgery to replicate the intended use of these models in a screening setting (**Supplementary Figure 1**). In the internal validation and internal held-out test sets, and all external validation sites, one ECG was randomly selected from one or more ECGs performed within 30 days of a TTE for each individual. In ELSA-Brasil, all participants who underwent both ECG and TTE at their baseline study visit were included.

SHD Outcome

The study outcome of SHD was defined as any LVSD, moderate-or-severe left-sided valve disease, or sLVH. All conditions were ascertained based on established guidelines from the cardiologist's interpretation of the TTE.[20] The left ventricular ejection fraction (LVEF) was primarily measured as a continuous variable using the biplane method. When the LVEF measurement using the biplane method was unavailable, measurements using the three-dimensional or visual estimation methods were used. LVSD was defined as an LVEF < 40%. Left-sided valve

diseases included aortic stenosis (AS), aortic regurgitation (AR), mitral regurgitation (MR), or mitral stenosis (MS), graded as mild to moderate, moderate, moderate to severe, or severe, based on established echocardiographic guidelines.[21,22] We defined sLVH by a combination of an interventricular septal diameter at end-diastole (IVSd) of greater than 15 mm, along with moderate to severe (grade II and grade III) LV diastolic dysfunction.[23]

Signal Processing and Image Generation

We used a strategy for developing models that can detect SHD from images from ECGs regardless of their layout. This was done using a custom waveform plotting strategy where ECG signals are processed and plotted as images in a format randomly chosen from 2880 formats, encapsulating variations in lead layouts, image color, lead label font, size and position, and grid and signal line width (**Supplementary Figure 2**). We also included non-conventional variations in ECG lead placements, with the chest leads on the left and limb leads on the right side of the plotted ECGs. The plotted signals were processed using a standard preprocessing strategy described previously (and included in **Supplemental Methods**). For evaluation, ECG images were plotted in standard clinical layout from signal waveform data, with a voltage calibration of 10 mm/mV, with the limbs and precordial leads arranged in four columns of 2.5-second each, representing leads I, II, and III; aVR, aVL, and aVF; V1, V2, and V3; and V4, V5, and V6 (**Supplementary Figure 3**). A 10-second recording of the lead I signal was included as a rhythm strip. We further evaluated the model on 4 novel image formats that were not encountered during model training (**Supplementary Methods**; **Supplementary Figure 4**). All images were converted to greyscale and down-sampled to 300x300 pixels using

Python Image Library.[24] Examples of ECG images in used for model training and

evaluation are presented in **Online Supplement 2**.

Model Development for Individual SHDs

We trained six independent CNN models to detect individual components of SHD.

We randomly divided individuals at YNHH into training, validation, and test sets

(85:5:10) without any patient spanning these sets (**Supplementary Figure 1**). We

retained multiple ECGs per person in the training set to ensure the adequacy of

training data. However, in evaluating the model in the internal validation, held-out

test, and external validation sets, only one ECG was randomly chosen for every

individual. Of note, none of the patients in the external validation sets were in the

model development population.

We used CNN models built upon the EfficientNet-B3 architecture, which has

384 layers and over 10 million trainable parameters.[11,25] To enable label-efficient

model development, we initialized the CNNs with weights from a model pretrained to

recognize individual patient-specific patterns in ECGs, independent of their

interpretation, using a self-supervised, contrastive learning framework (**Figure 1**).[26]

None of the ECGs on the self-supervised pretraining task represented individuals in

the SHD model development.

Each ECG in the training set was plotted using one of the randomly assigned

plotting formats described above. We used an Adam optimizer, gradient clipping,

and a minibatch size of 128 throughout training, with sequential unfreezing of the

final layers (learning rate, 0.001), and all layers (learning rate, 10^{-5}), with training

stopped when validation loss did not improve in 5 consecutive epochs. A custom

class-balanced loss function (weighted binary cross-entropy) based on the effective

number of samples was used, given the case and control imbalance.

The CNNs for the individual components of SHD had the same model

backbone but differed in the populations for training. Five of the six models,

specifically for those detecting LVSD, the presence of any moderate to severe left-

sided valvular heart diseases, and those for moderate-to-severe AR, AS, or MR,

were trained using all ECGs in the training set, spanning those with and without each

disease. However, given the low prevalence of sLVH (<1%), we age- and sex-

matched cases and controls for model development. Each case, representing an

ECG corresponding to an individual with sLVH, was matched to 10 control ECGs

without sLVH from someone of the same sex and within 5 years of age as the case.

These individual models were combined in an ensemble model to detect the

presence of any SHD. As a sensitivity analysis, we used the same training strategy

and model architecture to develop a classifier CNN model directly detecting the

presence of SHD. For each SHD component, we also trained corresponding signal-

based models within the same label and training population (**Supplementary**

Methods).

Ensemble Learning Strategy

Following CNN development, output probabilities from the 6 component SHD CNN

models, along with a person's age and sex, were used as input features for an

extreme gradient boosting (XGBoost) model, PRESENT-SHD (Practical scREening

using ENsemble machine learning sTrategy for SHD detection; **Figure 1**). The

XGBoost model was exclusively trained using data from the same training sets as

the CNN models. Before being included as features, age and the CNN model output

probabilities were standardized to a mean of 0 and a variance of 1 to improve

learning stability and ensure consistent feature contribution across different datasets.

To prevent data leakage, standardization at the time of inference in the testing sets

was done based on the distribution of these variables in the training set.

Prediction of new-onset SHD

To evaluate the use of the model for stratifying the risk of new-onset disease across

data sources, we identified a population without evidence of SHD or HF at baseline.

In YNHH, we identified the first recorded encounter for all individuals within the EHR

and instituted a 1-year blanking period to define prevalent diseases (**Supplementary

Figure 5**). Among 204,530 patients with ECGs following a one-year blanking period,

we excluded 6,909 individuals with prevalent SHD, 1,197 with a prior valvular repair

or replacement procedure, and 13,632 with prevalent HF (**Supplementary Table 1**).

Those included in the model training set (n = 55,245) were also excluded from this

analysis. We used a similar strategy across the hospital-based external validation

sites to identify patients at risk for new-onset disease – a one-year blanking period to

identify prevalent diseases and exclude those with prevalent SHD/HF, prior valvular

procedures. Across sets, new-onset SHD/HF was defined as the first occurrence of

any SHD detected on the TTE, any valvular replacement or repair procedure, or

hospitalization with HF. Data were censored at death or loss to follow-up.

Further, we identified participants with ECGs in the UKB. We used the

national EHR linkage to identify those who had not undergone any hospitalizations

with HF and had not undergone valvular procedures before their baseline ECG. We

followed these individuals till their first encounter with an SHD or HF diagnosis code

or a left-sided valve replacement or repair procedure (**Supplementary Table 1**).

Statistical Analysis

We reported continuous variables as median and interquartile range (IQR), and categorical variables as counts and percentages. Model performance for detecting SHD was reported as area under the receiver operating characteristic curve (AUROC) and area under the precision-recall curve (AUPRC), with 95% confidence intervals (CI) for these computed using bootstrapping with 1000 iterations. Additional performance measures included sensitivity, specificity, positive predictive value (PPV), negative predictive value (NPV), and F1 score with 95% CIs using the standard error formula for proportion. Finally, we calculated the model's PPV in simulated screening scenarios with different prevalences of composite SHD using the model's sensitivity and specificity corresponding to the probability threshold with sensitivity above 90% in the internal validation set.

Among those without SHD at baseline, the predictive role of PRESENT-SHD for new-onset SHD/HF was evaluated in age- and sex-adjusted Cox proportional hazard models. The time-to-first SHD/HF event was the dependent variable and the PRESENT-SHD-based screen status – presumably "false positive" or "true negative" status – was the key independent variable. Further, to account for the competing risk of death while evaluating new-onset SHD, we used age- and sex-adjusted multi-outcome Fine-Gray subdistribution hazard models.[28] The discrimination of the model for SHD prediction was assessed using Harrell's C-statistic.[29,30] The statistical analyses were two-sided, and the significance level was set at 0.05. Analyses were executed using Python 3.11.2 and R version 4.2.0. Our study follows the Transparent Reporting of a multivariable prediction model for Individual Prognosis Or

Diagnosis + Artificial Intelligence (TRIPOD + AI) checklist from the EQUATOR

network (**Supplementary Table 2**).[31]

RESULTS

Study Population

There were 261,228 ECGs from 93,693 unique patients in the training set, and the

validation and internal held-out test sets had a single ECG per person from 5,512

and 11,023 patients, respectively (**Supplementary Figure 1**). The development

population (model training and validation sets) had a median age of 67.8 (IQR, 56.1-

78.3) years, 49,947 were (50.3%) women, 13,383 (13.8%) non-Hispanic Black, and

7,754 were (8.1%) Hispanic (**Supplementary Table 3**). In the development

population, 60,096 (22.5%) ECGs were paired with TTEs with an SHD, including

25,552 (9.5%) with LVSD, 42,989 (16.1%) with moderate or severe left-sided

valvular disease, and 1,004 (0.4%) with sLVH.

At the external hospital sites, 18,222 patients at Bridgeport Hospital, 4,720

patients at Greenwich Hospital, 17,867 patients at Lawrence + Memorial Hospital,

and 3,782 patients from Westerly Hospital were included (**Supplementary Figure

1**), with 44,591 ECGs, randomly one chosen per person, across these sites for

model evaluation. Across hospital sites, the median age at ECG ranged from 66 to

74 years, with cohorts comprising 48.3% to 50.5% women, 1.5% to 19.4% Black,

and 1.4% to 15.9% Hispanic individuals. The distribution of SHDs across these

cohorts are described in **Supplementary Table 4**.

Of the 15,105 participants in ELSA-Brasil, 3,014 who underwent ECG and

TTE during their baseline visit were included. The median age of the cohort was 62.0

(IQR, 57.0-67.0) years, 1,596 (53.0%) were women, 1,661 (55.1%) were White, 455

(15.1%) were Black, and 753 (25.0%) were Pardo (or mixed race) individuals. A total of 88 (2.9%) individuals had SHD, with 37 (1.2%) with LVSD, 55 (1.8%) with moderate or severe left-sided valvular disease, and 6 (0.2%) with sLVH (**Supplementary Table 4**).

Detection of Structural Heart Disease

The ensemble XGBoost model, PRESENT-SHD, demonstrated an AUROC of 0.886 (95% CI, 0.877-0.894) and an AUPRC of 0.807 (95% CI, 0.791-0.823) for the detection of the composite SHD outcome in the held-out test set (**Table 1**). At the probability threshold for sensitivity above 90% in the internal validation set, the model had a sensitivity of 89.8% (95% CI, 89.0-90.5), specificity of 66.2% (95% CI, 65.0-67.4), PPV of 57.4% (95% CI, 56.1-58.6), and NPV of 92.8% (95% CI, 92.1-93.4) for detecting SHD in the held-out test set in YNHH (**Table 2; Supplementary Figure 6**). PRESENT-SHD performed consistently across subgroups of age, sex, race, and ethnicity (**Table 1**), and generalized well to novel ECG formats not encountered during training (**Supplementary Table 5**). Moreover, the model had consistent performance across subsets where TTEs were performed before, on the same day as, or after the ECG (**Supplementary Table 6**) and had high discrimination for detection of the severe SHD phenotype (LVSD, severe left-sided valve disease, or sLVH; **Supplementary Figure 7**). Notably, the performance of PRESENT-SHD was higher than the CNN models trained to directly detect SHD and other XGBoost ensemble strategies (**Supplementary Tables 7 and 8**). PRESENT-SHD performance was similar to the corresponding signal-based model for detecting SHD (**Supplementary Table 9**).

Further, PRESENT-SHD generalized well to the external validation cohorts at Bridgeport (AUROC, 0.854 [95% CI, 0.847-0.862]), Greenwich (AUROC, 0.900 [95% CI, 0.888-0.913]), Lawrence + Memorial (AUROC, 0.871 [95% CI, 0.864-0.878]), and Westerly (AUROC, 0.887 [95% CI, 0.874-0.902]) Hospitals, with sensitivities and specificities ranging 88-96% and 51-66%, respectively. PRESENT-SHD also generalized well to the population-based ELSA-Brasil, with an AUROC of 0.853 (95% CI: 0.811-0.897) and a sensitivity and specificity of 87.5% and 61.9%, respectively (**Table 2**). Across validation sites, model performance was consistent across demographic subgroups (**Supplementary Tables 10-14**). The F1 scores, PPVs, and NPVs for a range of putative prevalences of SHDs representing different screening scenarios are presented in **Supplementary Table 15**.

Detection of Individual Diseases

The models for LVSD, moderate or severe valvular disease, and sLVH had AUROCs of 0.914 (95% CI, 0.904-0.924), 0.805 (95% CI, 0.793-0.817), and 0.903 (95% CI, 0.850-0.946; **Figure 2**), respectively. The performance of CNN models for individual valvular heart diseases varied, with an AUROC of 0.722 (95% CI, 0.784-0.824) for moderate or severe AR, 0.804 (95% CI, 0.784-0.824) for AS, and 0.792 (95% CI, 0.776-0.807) for MR. The CNN model AUPRCs varied with individual disease prevalence (**Supplementary Tables 16-21**). The performance for individual disease CNNs was consistent across external validation cohorts (**Supplementary Figure 8; Supplementary Tables 16-21**).

Prediction of SHD and Cardiovascular Risk

Of the 127,547 individuals at risk in YNHH, 5,346 (4.2%) had new-onset SHD/HF

over a median of 4.0 (IQR 1.7-6.4) years of follow-up. Across the hospital-based

external validation sites, there were 63,748 individuals without SHD/HF at baseline

and 4,593 (7.2%) developed incident SHD/HF over a median of 3.1 years (IQR, 1.3-

5.0) of follow up (**Supplementary Table 22**). In UKB, 413 (1.0%) of 41,800

individuals developed SHD/HF over 3.0 (IQR 2.1-4.5) years of follow-up.

A positive PRESENT-SHD screen portended a 4-fold higher risk of new-onset

SHD/HF in YNHH (age- and sex-adjusted HR [aHR], 4.28 [95% CI, 3.95-4.64],

Harrell's C-statistic, 0.823 [95% CI, 0.817-0.828]) and every 10% increment in model

probability was progressively associated with a 36% higher hazard for incident

SHD/HF (aHR, 1.36 [1.35-1.38]). A similar pattern was observed across all external

validation hospital sites (**Supplementary Tables 23 and 24**). This association

remained consistent after adjusting for comorbidities at baseline and the competing

risk of death (**Supplementary Table 23**).

In the UKB, a positive vs. negative PRESENT-SHD screen was associated

with twice the hazard of developing SHD/HF (aHR, 2.39 [95% CI, 1.87-3.04],

Harrell's C-statistic, 0.754 [95% CI, 0.728-0.780]). Across all sites, higher model

probabilities were associated with progressively higher risk of new-onset SHD/HF

(**Supplementary Table 25; Figure 3**).

DISCUSSION

We developed and validated PRESENT-SHD, an ensemble deep learning model that

uses an ECG image as the input to detect a range of SHDs. PRESENT-SHD had

excellent performance in detecting SHDs across five distinct US hospitals with

unique patients and in a population-based cohort study from Brazil. Model

performance was consistent across demographic subgroups and similar to the corresponding signal-based models. Further, in individuals without SHD at baseline, PRESENT-SHD identified those with an up to 4-fold higher risk of developing new-onset SHD/HF, across both health system-centered cohorts in the US and in a community-based cohort in the UK. The model was well calibrated to the risk of new-onset disease, such that higher PRESENT-SHD probabilities were associated with progressively higher risk of developing SHD/HF. Thus, an image-based AI-ECG approach is a scalable and accessible strategy for screening for SHDs and identifying those at high risk for developing SHDs.

Prior studies have reported the use of deep learning on 12-lead ECGs to detect individual structural cardiovascular conditions, including LVSD,[10,11,13] hypertrophic cardiomyopathy,[16,32,33] cardiac amyloidosis,[34,35] aortic stenosis,[12] among others.[15,35–37] While these models provide a strong foundation for the role of ECG-based detection of SHDs, the low prevalence of these individual diseases, their potential implementation for broad screening is limited by the low PPVs of the proposed models.[10–12,16,32–34] The simultaneous detection of multiple SHDs increases the composite disease prevalence and improves model precision[19] Through a focus on detecting any of the clinically relevant SHDs that require TTE for confirmation, PRESENT-SHD enables efficient screening by limiting false discovery. Moreover, the direct use of ECG images as the input, and a flexible strategy that allows for varying formats, supports the scalability of the approach across resources settings.[38]

Our work has additional features that build upon the studies reported in the literature. A focus on developing PRESENT-SHD in diverse populations enabled its consistent performance in demographic subgroups across validation sites. Moreover, in addition to the accurate detection of cross-sectional disease, PRESENT-SHD also

predicted the risk of new-onset disease in those without baseline SHD, representing a novel strategy for cardiovascular risk stratification. The model was well calibrated to predict the risk of SHD, suggesting that those with high PRESENT-SHD scores can benefit from surveillance, evaluation, and management of risk factors.[7,39–41]

The application of PRESENT-SHD has important implications for cardiovascular screening. Since early disease detection and intervention can alter the trajectory and outcomes of patients with SHDs, an AI-ECG-based approach that leverages ECG images can enable opportunistic screening through automated deployment across clinical settings where ECGs are obtained.[42,43] The focus on a composite model that detects a broad range of SHDs simultaneously reduces the burden of false positive screens and downstream testing, which is a major concern for AI-ECG models developed for individual cardiovascular conditions. This high PPV can allow for a sensitive threshold to be selected during implementation to identify those who should be referred for further imaging. Given that the individual components of SHD share a common diagnostic test, a TTE, screening with PRESENT-SHD can help triage the use of TTE testing. Those with a positive AI-ECG screen can be prioritized for cardiac imaging, which is especially helpful in settings where access may be limited.[1,38,44]

Our study has limitations that merit consideration. First, the development population represented a selected set of patients with a clinical indication for an ECG and a TTE. The consistent validation of the model across populations with a broad range of clinical subpopulations seen in community as well as referral hospitals suggests that the model learned generalizable signatures of the SHDs. This is further supported by the consistent validation of PRESENT-SHD in the ELSA-Brasil study, where individuals underwent protocolized ECGs and echocardiograms

concurrently at enrollment without any confounding by indication. Nonetheless,
continued prospective validation studies are necessary before broad use in a
screening population. Second, although we developed the model using a novel
approach that generates a broad range of ECG image formats and demonstrated
consistent performance across previously unseen formats, further evaluation of
PRESENT-SHD with scanned ECG images and photographs, along with
implementing image quality control measures, is necessary before wider clinical use.
Third, while we used age- and sex-matched controls for the development of the CNN
model for sLVH detection, we did not evaluate alternative approaches that
additionally use clinical risk factors for case-control matching.

Fourth, although the development of the model focused on plotted images,
the signal preprocessing before image plotting represented standard steps used in
ECG machines before ECG images are generated or printed. Thus, any processing
of ECG images is not required for the real-world application of PRESENT-SHD, as
also demonstrated in the publicly accessible application of the model. Fifth, model
performance was lower in individuals aged 65 and older, potentially limiting reliability
as a standalone tool to rule out the need for cardiac imaging. Adjusting model
thresholds or developing age-specific models could be evaluated to improve
performance. Sixth, we did not evaluate the cost-effectiveness of PRESENT-SHD
use in clinical settings. However, the model had a high PPV for cross-sectional
disease detection and identified individuals at high risk of developing SHD/HF,
representing features favorable for deployment. Finally, in the predictive evaluation
of the model, despite broad geographic coverage, some outcome events may have
occurred outside the YNHH and the community hospitals, potentially resulting in
incomplete capture of longitudinal outcomes. Nonetheless, the model risk

stratification was consistent in the UKB, where the ECGs were protocolized and
outcomes were ascertained using national EHR linkage.

CONCLUSION

We developed and validated a novel approach for the detection and the prediction of
a range of SHDs using images of 12-lead ECGs, representing a scalable and
accessible tool for SHD screening and risk stratification.

Conflict of Interest Disclosures

Dr. Khera is an Associate Editor of JAMA. Dr. Khera and Mr. Sangha are the
coinventors of U.S. Provisional Patent Application No. 63/346,610, "Articles and
methods for format-independent detection of hidden cardiovascular disease from
printed electrocardiographic images using deep learning" and are co-founders of
Ensight-AI. Dr. Khera receives support from the National Institutes of Health (under
awards R01AG089981, R01HL167858, and K23HL153775) and the Doris Duke
Charitable Foundation (under award 2022060). He receives support from the
Blavatnik Foundation through the Blavatnik Fund for Innovation at Yale. He also
receives research support, through Yale, from Bristol-Myers Squibb, BridgeBio, and
Novo Nordisk. In addition to 63/346,610, Dr. Khera is a coinventor of U.S. Pending
Patent Applications WO2023230345A1, US20220336048A1, 63/484,426,
63/508,315, 63/580,137, 63/606,203, 63/619,241, and 63/562,335. Dr. Khera and
Dr. Oikonomou are co-founders of Evidence2Health, a precision health platform to
improve evidence-based cardiovascular care. Dr. Oikonomou has been a consultant
for Caristo Diagnostics Ltd and Ensight-AI Inc, and has received royalty fees from
technology licensed through the University of Oxford, outside the submitted work. Dr.

Data Sharing Statement

Data from the UK Biobank and the Brazilian Longitudinal Study of Adult Health are available for research to licensed users. Individual-level data for the Yale New Haven

Health System cannot be made available due to HIPAA regulations enforced by the

Yale IRB. The model is publicly accessible for research use on our website and

programming code for generating key results is available from the authors on

request.

REFERENCES

1. Steinberg DH, Staubach S, Franke J, Sievert H. Defining structural heart disease in the adult patient: current scope, inherent challenges and future directions. *Eur Heart J Suppl.* 2010;12:E2–E9.

2. Picano E. Economic and biological costs of cardiac imaging. *Cardiovasc Ultrasound.* 2005;3.

3. Vitola JV, Shaw LJ, Allam AH, et al. Assessing the need for nuclear cardiology and other advanced cardiac imaging modalities in the developing world. *J Nucl Cardiol.* 2009;16:956–961.

4. Alkhouli M, Alqahtani F, Holmes DR, Berzingi C. Racial disparities in the utilization and outcomes of structural heart disease interventions in the United States. *J Am Heart Assoc.* 2019;8.

5. Samad Z, Sivak JA, Phelan M, Schulte PJ, Patel U, Velazquez EJ. Prevalence and outcomes of left-sided valvular heart disease associated with Chronic kidney disease. *J Am Heart Assoc.* 2017;6.

6. Fleury M-A, Clavel M-A. Sex and race differences in the pathophysiology, diagnosis, treatment, and outcomes of valvular heart diseases. *Can J Cardiol.* 2021;37:980–991.

7. Baumgartner H, Iung B, Otto CM. Timing of intervention in asymptomatic patients with valvular heart disease. *Eur Heart J.* 2020;41:4349–4356.

8. Wang TJ, Evans JC, Benjamin EJ, Levy D, LeRoy EC, Vasan RS. Natural history of asymptomatic left ventricular systolic dysfunction in the community. *Circulation*. 2003;108:977–982.

9. Galasko GI, Barnes SC, Collinson P, Lahiri A, Senior R. What is the most cost-effective strategy to screen for left ventricular systolic dysfunction: natriuretic peptides, the electrocardiogram, hand-held echocardiography, traditional echocardiography, or their combination? *Eur Heart J*. 2006;27:193–200.

10. Attia ZI, Kapa S, Lopez-Jimenez F, et al. Screening for cardiac contractile dysfunction using an artificial intelligence-enabled electrocardiogram. *Nat Med*. 2019;25:70–74.

11. Sangha V, Nargesi AA, Dhingra LS, et al. Detection of Left Ventricular Systolic Dysfunction From Electrocardiographic Images. *Circulation*. 2023. Published onlineJuly 25, 2023. https://doi.org/10.1161/CIRCULATIONAHA.122.062646.

12. Cohen-Shelly M, Attia ZI, Friedman PA, et al. Electrocardiogram screening for aortic valve stenosis using artificial intelligence. *Eur Heart J*. 2021;42:2885–2896.

13. Bjerkén LV, Rønborg SN, Jensen MT, Ørting SN, Nielsen OW. Artificial intelligence enabled ECG screening for left ventricular systolic dysfunction: a systematic review. *Heart Fail Rev*. 2023;28:419–430.

14. Khunte A, Sangha V, Oikonomou EK, et al. Detection of left ventricular systolic dysfunction from single-lead electrocardiography adapted for portable and wearable devices. *NPJ Digit Med*. 2023;6:124.

15. Oikonomou EK, Sangha V, Dhingra LS, et al. Artificial intelligence-enhanced risk stratification of cancer therapeutics-related cardiac dysfunction using electrocardiographic images. *bioRxiv*. 2024:2024.03.12.24304047.

16. Sangha V, Dhingra LS, Oikonomou EK, et al. Identification of hypertrophic cardiomyopathy on electrocardiographic images with deep learning. *medRxiv*. 2023:2023.12.23.23300490.

17. Dhingra LS, Sangha V, Aminorroaya A, et al. A multicenter evaluation of the impact of procedural and pharmacological interventions on deep learning-based electrocardiographic markers of hypertrophic cardiomyopathy. *bioRxiv*. 2024.

18. Dhingra LS, Aminorroaya A, Camargos AP, et al. Using artificial intelligence to predict heart failure risk from single-lead electrocardiographic signals: A multinational assessment. *bioRxiv*. 2024:2024.05.27.24307952.

19. Ulloa-Cerna AE, Jing L, Pfeifer JM, et al. rECHOmmend: An ECG-Based Machine Learning Approach for Identifying Patients at Increased Risk of Undiagnosed Structural Heart Disease Detectable by Echocardiography. *Circulation*. 2022;146:36–47.

20. Mitchell C, Rahko PS, Blauwet LA, et al. Guidelines for performing a comprehensive transthoracic echocardiographic examination in adults: Recommendations from the American society of echocardiography. *J Am Soc Echocardiogr*. 2019;32:1–64.

21. Zoghbi WA, Adams D, Bonow RO, et al. Recommendations for noninvasive evaluation of native valvular regurgitation: A report from the American society of

echocardiography developed in collaboration with the society for cardiovascular magnetic resonance. *J Am Soc Echocardiogr.* 2017;30:303–371.

22. Zoghbi WA, Adams D, Bonow RO, et al. Recommendations for noninvasive evaluation of native valvular regurgitation. *J Indian Acad Echocardiogr Cardiovasc Imaging.* 2020;4:58–121.

23. Kossaify A, Nasr M. Diastolic dysfunction and the new recommendations for echocardiographic assessment of left ventricular diastolic function: Summary of guidelines and novelties in diagnosis and grading. *J Diagn Med Sonogr.* 2019;35:317–325.

24. Anon. Pillow. *PyPI* Accessed February 29, 2024. https://pypi.org/project/pillow/.

25. Anon. Mingxing Tan and Quoc V Le. EfficientNet: Rethinking model scaling for convolutional neural networks. *International Conference on Machine Learning, 2019*

26. Sangha V, Khunte A, Holste G, et al. Biometric contrastive learning for data-efficient deep learning from electrocardiographic images. *J Am Med Inform Assoc.* 2024. Published onlineJanuary 24, 2024. https://doi.org/10.1093/jamia/ocae002.

27. Austin PC, Fine JP. Practical recommendations for reporting Fine-Gray model analyses for competing risk data. *Stat Med.* 2017;36:4391–4400.

28. Uno H, Cai T, Pencina MJ, D'Agostino RB, Wei LJ. On the C-statistics for evaluating overall adequacy of risk prediction procedures with censored survival data. *Stat Med.* 2011;30:1105–1117.

29. Kang L, Chen W, Petrick NA, Gallas BD. Comparing two correlated C indices with right-censored survival outcome: a one-shot nonparametric approach. *Stat Med.* 2015;34:685–703.

30. Anon. TRIPOD+AI statement: updated guidance for reporting clinical prediction models that use regression or machine learning methods. *BMJ.* 2024;385:q902.

31. Ko W-Y, Siontis KC, Attia ZI, et al. Detection of Hypertrophic Cardiomyopathy Using a Convolutional Neural Network-Enabled Electrocardiogram. *J Am Coll Cardiol.* 2020;75:722–733.

32. Goto S, Solanki D, John JE, et al. Multinational Federated Learning Approach to Train ECG and Echocardiogram Models for Hypertrophic Cardiomyopathy Detection. *Circulation.* 2022;146:755–769.

33. Grogan M, Lopez-Jimenez F, Cohen-Shelly M, et al. Artificial intelligence–enhanced electrocardiogram for the early detection of cardiac amyloidosis. *Mayo Clin Proc.* 2021;96:2768–2778.

34. Taborsky M, Aiglova R, Fedorco M, et al. Detection of arrhythmias in patients with cardiac amyloidosis using implantable ECG recorders. *Eur Heart J.* 2022;43.

35. Duong SQ, Vaid A, Vy HMT, et al. Quantitative prediction of right ventricular and size and function from the electrocardiogram. *medRxiv.* 2023. Published onlineApril 26, 2023. https://doi.org/10.1101/2023.04.25.23289130.

36. Vaid A, Johnson KW, Badgeley MA, et al. Using Deep-Learning Algorithms to Simultaneously Identify Right and Left Ventricular Dysfunction From the Electrocardiogram. *JACC Cardiovasc Imaging.* 2022;15:395–410.

37. Oikonomou EK, Sangha V, Shankar SV, et al. Tracking the pre-clinical progression of transthyretin amyloid cardiomyopathy using artificial intelligence-enabled electrocardiography and echocardiography. *bioRxiv*. 2024:2024.08.25.24312556.

38. Mocumbi AO. Cardiovascular health care in low- and middle-income countries. *Circulation*. 2024;149:557–559.

39. Tarakji KG, Brunken R, McCarthy PM, et al. Myocardial viability testing and the effect of early intervention in patients with advanced left ventricular systolic dysfunction. *Circulation*. 2006;113:230–237.

40. Ullah W, Gowda SN, Khan MS, et al. Early intervention or watchful waiting for asymptomatic severe aortic valve stenosis: a systematic review and meta-analysis. *J Cardiovasc Med (Hagerstown)*. 2020;21:897–904.

41. Levin A, Singer J, Thompson CR, Ross H, Lewis M. Prevalent left ventricular hypertrophy in the predialysis population: identifying opportunities for intervention. *Am J Kidney Dis*. 1996;27:347–354.

42. Topol E. Opportunistic A.i. for medical scans. *Ground Truths*. 2024. Accessed July 28, 2024. https://erictopol.substack.com/p/opportunistic-ai-for-medical-scans.

43. Jelinek H, Warner P, King S, De Jong B. Opportunistic screening for cardiovascular problems in rural and remote health settings. *J Cardiovasc Nurs*. 2006;21:217–222.

44. Diamantino AC, Nascimento BR, Nunes MCP, et al. Impact of incorporating

echocardiographic screening into a clinical prediction model to optimise utilisation of

echocardiography in primary care. *Int J Clin Pract*. 2021;75:e13686.

Figure 1. Model Development Strategy and Study Design. Abbreviations: AR, aortic regurgitation; AS, aortic stenosis; CNN, convolutional neural network; ECG, electrocardiogram; FC, fully-connected layers; LVSD, left ventricular systolic dysfunction; MR, mitral regurgitation; SHD, structural heart diseases; sLVH, severe left ventricular hypertrophy; TTE, transthoracic echocardiogram; XGBoost, extreme gradient boosting
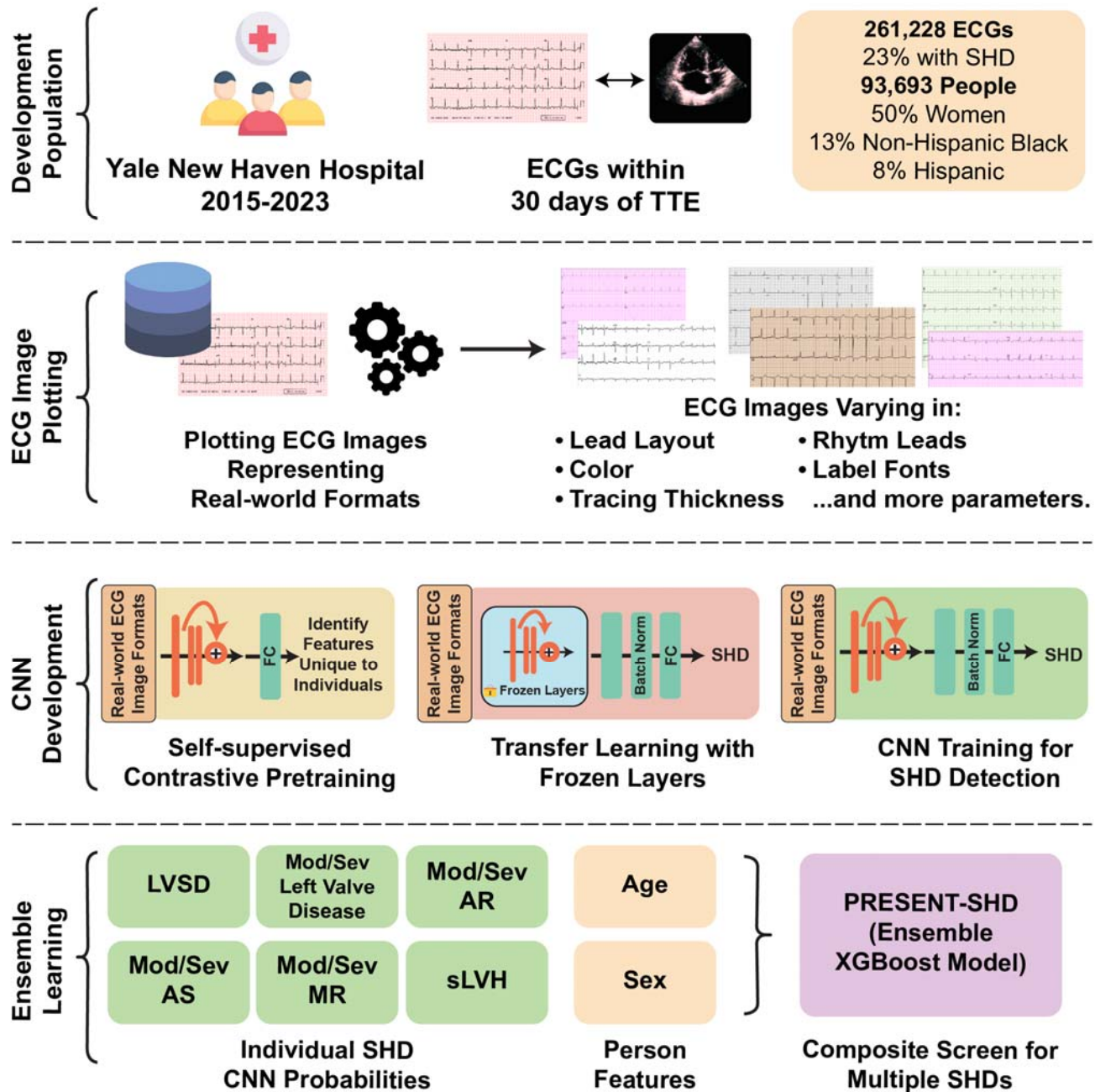
Figure 2. Model discrimination for the detection of composite structural heart disease and individual components in the held-out test set. Abbreviations: AR, aortic regurgitation; AS, aortic stenosis; CI, confidence intervals; LVEF, left ventricular ejection fraction; LVH, severe left ventricular hypertrophy; LVSD, left ventricular systolic dysfunction; MR, mitral regurgitation; SHD, structural heart diseases
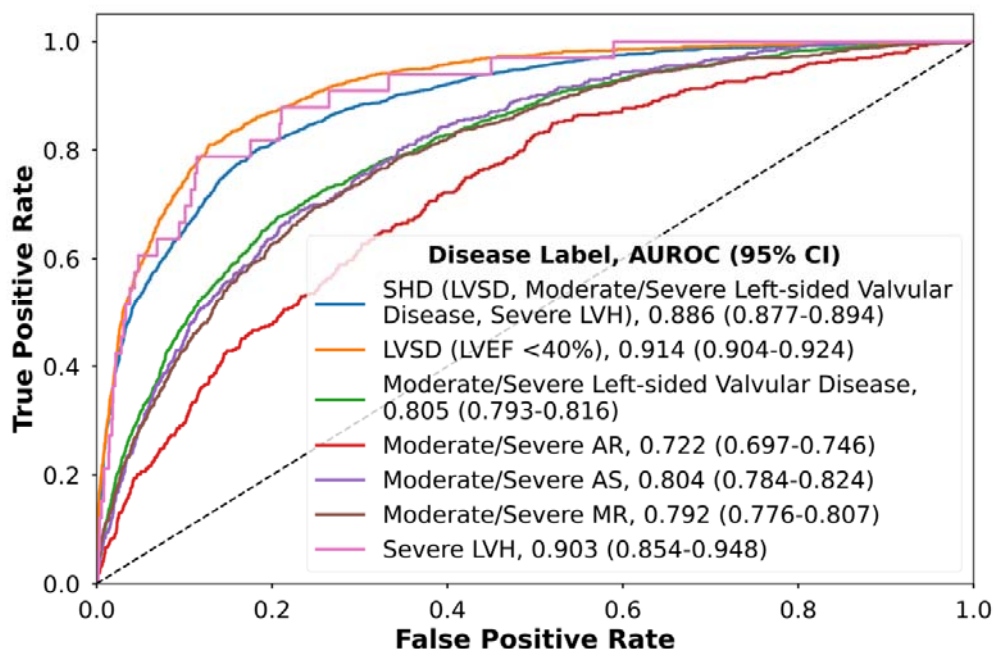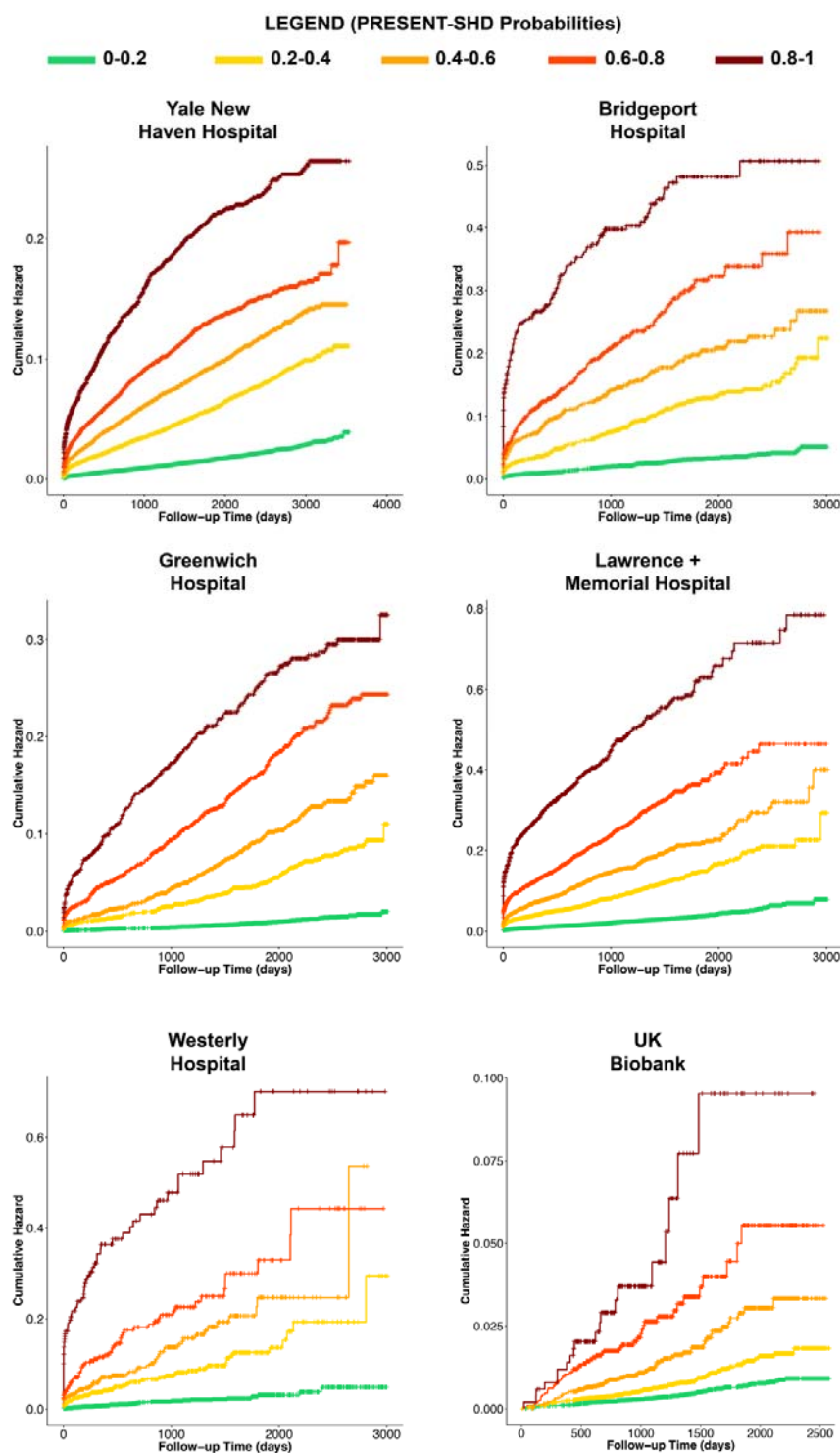
Figure 3. Cumulative hazard for new-onset structural heart disease or heart failure hospitalization in individuals without structural heart disease or heart failure at baseline.

*Footnote: The scale of the y-axes varies across cohorts.

Table 1. Performance metrics for detecting structural heart disease across demographic subgroups in the held-out test set.
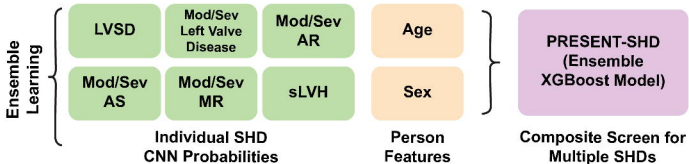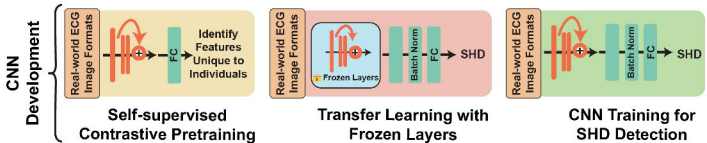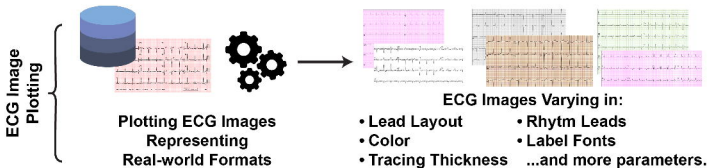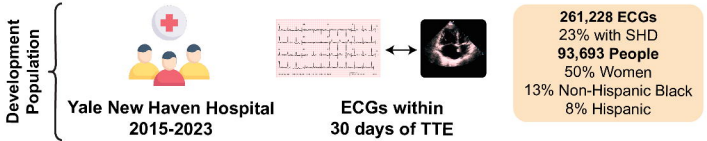Abbreviations: AUPRC, area under the precision-recall curve; AUROC, area under the receiver operating characteristic curve; NPV, negative predictive value; PPV, positive predictive value.

Subgroup	Total Number	Diagnostic OR	AUROC	AUPRC	F1 Score	Prevalence	Sensitivity	Specificity	PPV	NPV
Overall	6203	17.2 (14.7-20.1)	0.886 (0.877-0.894)	0.807 (0.791-0.823)	0.7	33.60%	89.8% (89.0-90.5)	66.2% (65.0-67.4)	57.4% (56.1-58.6)	92.8% (92.1-93.4)
Age ≥ 65 years	2897	8.0 (6.1-10.5)	0.822 (0.807-0.838)	0.839 (0.820-0.857)	0.735	53.20%	95.7% (94.9-96.4)	26.6% (25.0-28.2)	59.7% (57.9-61.5)	84.3% (83.0-85.7)
Age < 65 years	3306	16.2 (13.1-20.2)	0.873 (0.856-0.889)	0.679 (0.641-0.716)	0.595	16.50%	73.2% (71.7-74.7)	85.6% (84.4-86.8)	50.1% (48.4-51.8)	94.2% (93.4-95.0)
Women	3150	17.5 (14.1-21.7)	0.884 (0.873-0.896)	0.778 (0.752-0.804)	0.689	30.80%	88.5% (87.3-89.6)	69.5% (67.9-71.1)	56.4% (54.7-58.1)	93.1% (92.2-94.0)
Men	3052	16.7 (13.3-20.9)	0.886 (0.874-0.898)	0.830 (0.810-0.851)	0.71	36.50%	90.9% (89.9-92.0)	62.4% (60.7-64.2)	58.2% (56.4-59.9)	92.3% (91.3-93.2)
Non-Hispanic White	3966	16.7 (13.7-20.5)	0.882 (0.871-0.892)	0.824 (0.805-0.841)	0.711	37.40%	91.7% (90.9-92.6)	60.2% (58.7-61.7)	58.0% (56.4-59.5)	92.4% (91.6-93.2)
Non-Hispanic Black	834	17.2 (11.4-25.9)	0.877 (0.852-0.902)	0.774 (0.724-0.823)	0.697	31.50%	87.8% (85.6-90.1)	70.4% (67.3-73.5)	57.8% (54.4-61.1)	92.6% (90.9-94.4)
Hispanic	537	15.8 (9.7-25.8)	0.882 (0.846-0.916)	0.786 (0.720-0.844)	0.666	25.50%	81.0% (77.7-84.3)	78.8% (75.3-82.2)	56.6% (52.4-60.8)	92.4% (90.1-94.6)
Others	866	18.1 (11.9-27.5)	0.893 (0.868-0.918)	0.740 (0.668-0.803)	0.648	23.10%	84.0% (81.6-86.4)	77.5% (74.7-80.3)	52.8% (49.5-56.2)	94.2% (92.6-95.7)

Table 2. Model performance characteristics for PRESENT-SHD for detection of structural heart disease across the held-out test set and external validation cohorts.

Abbreviations: AUPRC, area under the precision recall curve; AUROC, area under the receiver operating characteristic curve; NPV, negative predictive value; PPV, positive predictive value.
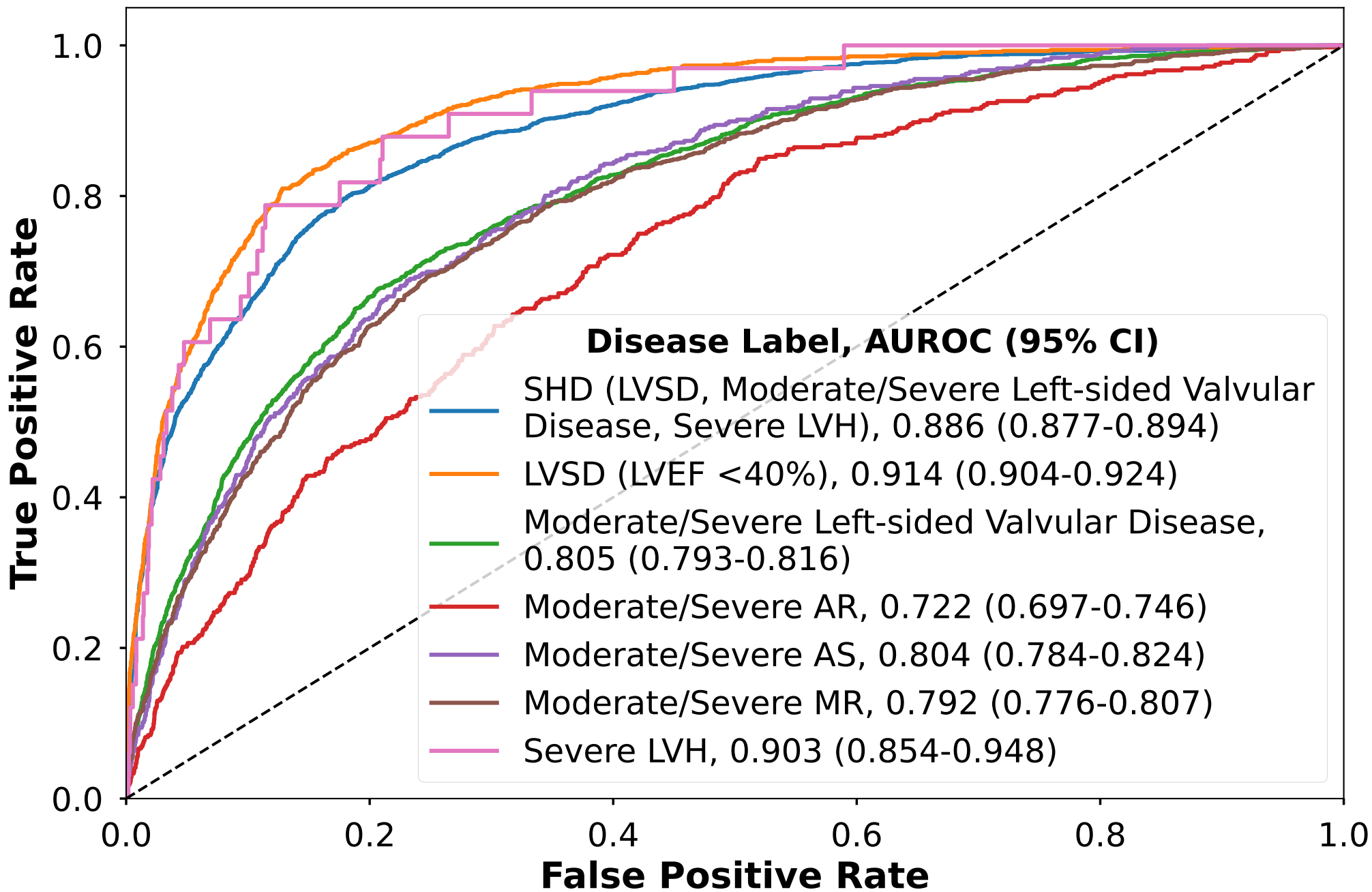
| Cohort Type	Site Name	Total Number	Diagnostic OR	AUROC	AUPRC	F1 Score	Prevalence	Sensitivity	Specificity	PPV	NPV
Held-out test set	**Yale New Haven Hospital**	6203	17.2 (14.7-20.1)	0.886 (0.877-0.894)	0.807 (0.791-0.823)	0.7	33.60%	89.8% (89.0-90.5)	66.2% (65.0-67.4)	57.4% (56.1-58.6)	92.8% (92.1-93.4)
External validation – Hospital sites	**Bridgeport Hospital**	8944	14.8 (12.9-16.9)	0.854 (0.847-0.862)	0.834 (0.823-0.845)	0.751	46.60%	93.2% (92.6-93.7)	52.0% (51.0-53.1)	62.9% (61.9-63.9)	89.7% (89.1-90.3)
	Greenwich Hospital	2271	30.6 (22.2-42.1)	0.900 (0.888-0.913)	0.894 (0.878-0.910)	0.798	49.80%	96.0% (95.2-96.8)	55.9% (53.9-58.0)	68.3% (66.4-70.2)	93.4% (92.4-94.4)
	Lawrence + Memorial Hospital	11447	16.0 (14.0-18.2)	0.871 (0.864-0.878)	0.771 (0.757-0.784)	0.643	31.50%	92.5% (92.0-93.0)	56.4% (55.5-57.3)	49.3% (48.4-50.3)	94.3% (93.8-94.7)
	Westerly Hospital	1843	19.9 (14.5-27.3)	0.887 (0.874-0.902)	0.906 (0.890-0.922)	0.81	55.60%	95.1% (94.1-96.1)	50.5% (48.3-52.8)	70.6% (68.6-72.7)	89.2% (87.8-90.6)
External validation – Population-based cohort	**ELSA-Brasil**	2988	11.4 (6.0-21.5)	0.853 (0.811-0.897)	0.354 (0.253-0.460)	0.121	2.90%	87.5% (86.3-88.7)	61.9% (60.2-63.6)	6.5% (5.6-7.4)	99.4% (99.1-99.7)

Development Population

Yale New Haven Hospital
2015-2023

ECGs within
30 days of TTE

261,228 ECGs
23% with SHD
93,693 People
50% Women
13% Non-Hispanic Black
8% Hispanic

ECG Image Plotting

Plotting ECG Images
Representing
Real-world Formats

ECG Images Varying in:
- Lead Layout
- Color
- Tracing Thickness
- Rhytm Leads
- Label Fonts
- ...and more parameters.

CNN Development

Real-world ECG Image Formats → FC → Identify Features Unique to Individuals

**Self-supervised
Contrastive Pretraining**

Real-world ECG Image Formats → Frozen Layers → Batch Norm → FC → SHD

**Transfer Learning with
Frozen Layers**

Real-world ECG Image Formats → Batch Norm → FC → SHD

**CNN Training for
SHD Detection**

Ensemble Learning

LVSD	Mod/Sev Left Valve Disease	Mod/Sev AR	Age
Mod/Sev AS	Mod/Sev MR	sLVH	Sex

**Individual SHD
CNN Probabilities**

**Person
Features**

**PRESENT-SHD
(Ensemble
XGBoost Model)**

**Composite Screen for
Multiple SHDs**

Disease Label, AUROC (95% CI)

SHD (LVSD, Moderate/Severe Left-sided Valvular Disease, Severe LVH), 0.886 (0.877-0.894)

LVSD (LVEF <40%), 0.914 (0.904-0.924)

Moderate/Severe Left-sided Valvular Disease, 0.805 (0.793-0.816)

Moderate/Severe AR, 0.722 (0.697-0.746)

Moderate/Severe AS, 0.804 (0.784-0.824)

Moderate/Severe MR, 0.792 (0.776-0.807)

Severe LVH, 0.903 (0.854-0.948)

LEGEND (PRESENT-SHD Probabilities)

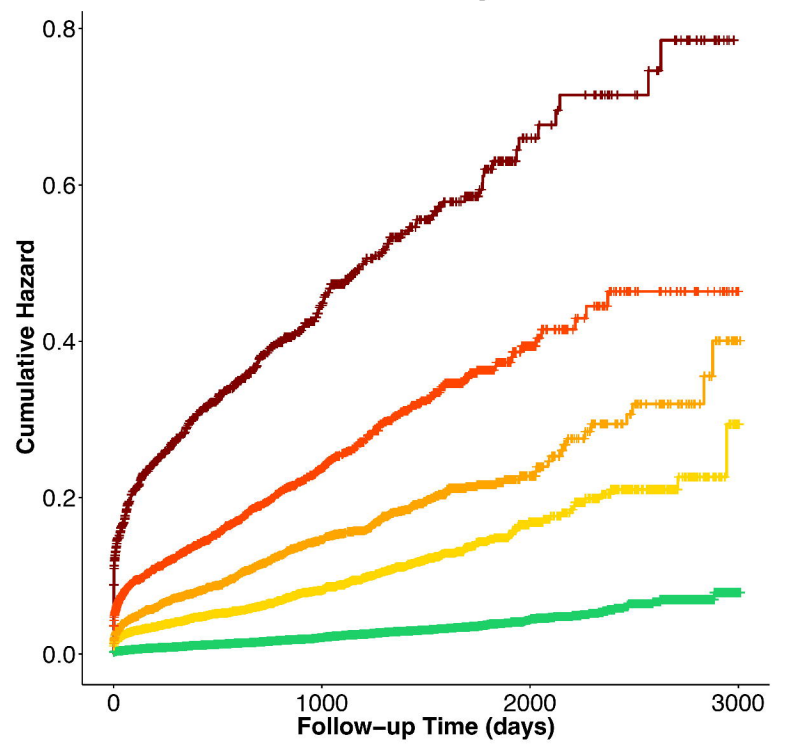| 0-0.2 | 0.2-0.4 | 0.4-0.6 | 0.6-0.8 | 0.8-1 |

Yale New Haven Hospital
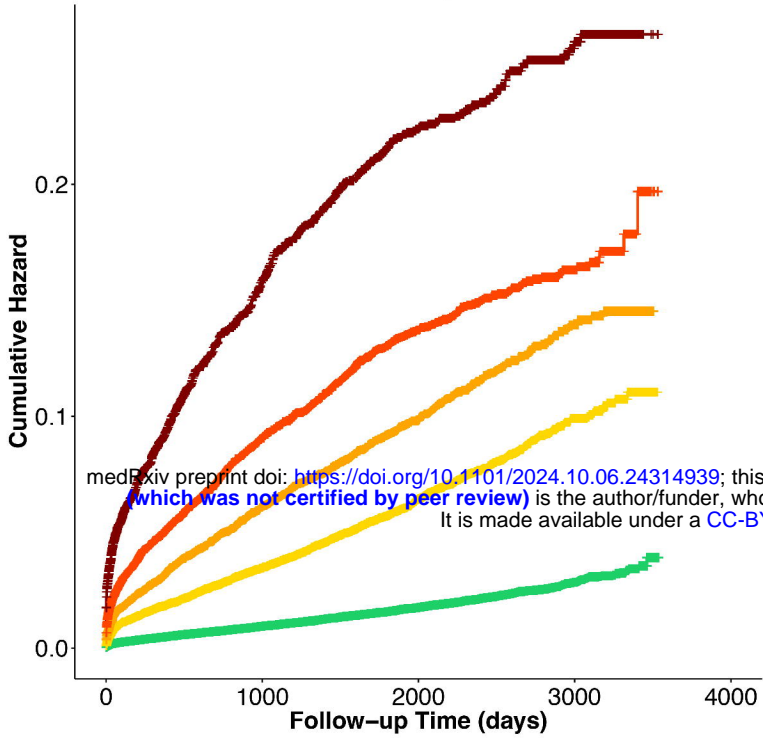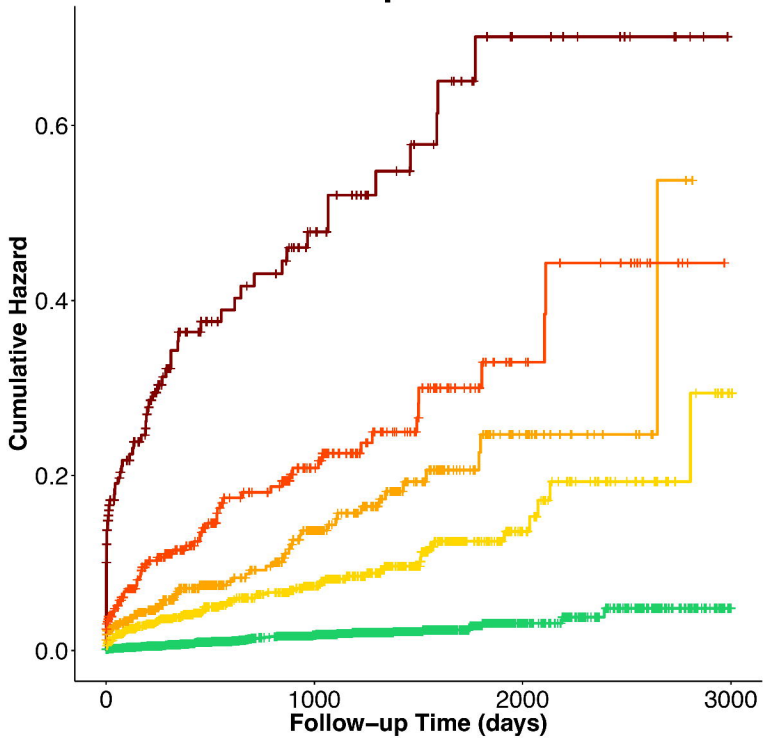
Bridgeport Hospital
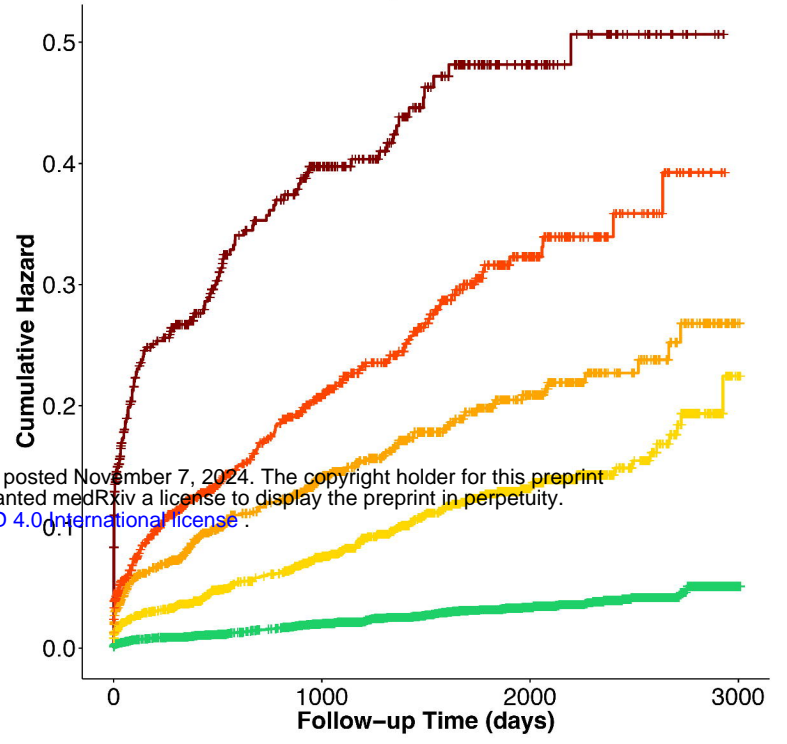
Greenwich Hospital
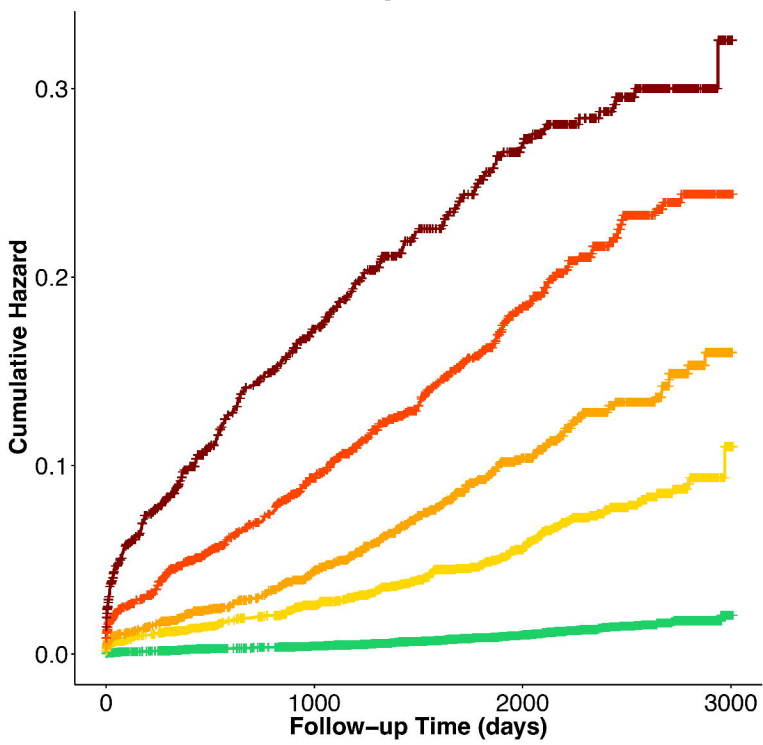
Lawrence + Memorial Hospital

Westerly Hospital

UK Biobank